

## Basic Study

## Mitochondrial pathway of the lysine demethylase 5C inhibitor CPI-455 in the Eca-109 esophageal squamous cell carcinoma cell line

Xiao-Jie Xue, Fei-Rong Li, Jing Yu

**ORCID number:** Xiao-Jie Xue 0000-0003-0315-1253; Fei-Rong Li 0000-0003-0166-8064; Jing Yu 0000-0001-5836-5334.

**Author contributions:** Xue XJ analyzed the data, drafted the article, and contributed to study design; Li FR contributed to data gathering; Yu J contributed to study design, editing, and revising the paper; all authors read and approved the final manuscript.

**Supported by** Young Talents Project of Hubei Provincial Health Commission, No. WJ2019H449.

**Institutional review board**

**statement:** The study was reviewed and approved by Hubei cancer hospital, Tongji Medical College, Huazhong University of Science and Technology (approval No. LLHBCH2020LW-027).

**Conflict-of-interest statement:** The authors declare that they have no competing interests..

**Data sharing statement:** No additional data are available.

**Open-Access:** This article is an open-access article that was selected by an in-house editor and fully peer-reviewed by external reviewers. It is distributed in accordance with the Creative

**Xiao-Jie Xue, Fei-Rong Li,** Department of Clinical Laboratory, Huangshi Central Hospital, Affiliated Hospital of Hubei Polytechnic University, Edong Healthcare Group, Huangshi 435000, Hubei Province, China

**Xiao-Jie Xue,** Hubei Key Laboratory of Kidney Disease Pathogenesis and Intervention, Huangshi 435000, Hubei Province, China

**Xiao-Jie Xue,** Medical College, Wuhan University of Science and Technology, Wuhan 430081, Hubei Province, China

**Jing Yu,** Department of Laboratory Medicine, Hubei Cancer Hospital, Tongji Medical College, Huazhong University of Science and Technology, Wuhan 430079, Hubei Province, China

**Corresponding author:** Jing Yu, PhD, Doctor, Department of Laboratory Medicine, Hubei Cancer Hospital, Tongji Medical College, Huazhong University of Science and Technology, No. 116 Zhuodaquan South Road, Wuhan 430079, Hubei Province, China.  
[yujings9774@sina.com.cn](mailto:yujings9774@sina.com.cn)

**Abstract****BACKGROUND**

Esophageal cancer is a malignant tumor of the digestive tract that is difficult to diagnose early. CPI-455 has been reported to inhibit various cancers, but its role in esophageal squamous cell carcinoma (ESCC) is unknown.

**AIM**

To investigate the effects and mechanism of the lysine demethylase 5C inhibitor, CPI-455, on ESCC cells.

**METHODS**

A methyl tetrazolium assay was used to detect the inhibitory effect of CPI-455 on the proliferation of Eca-109 cells. Apoptosis, reactive oxygen species (ROS), and mitochondrial membrane potential were assessed by flow cytometry. Laser confocal scanning and transmission electron microscopy were used to observe changes in Eca-109 cell morphology. The protein expression of P53, Bax, lysine-specific demethylase 5C (KDM5C), cleaved Caspase-9, and cleaved Caspase-3 were assayed by western blotting.

**RESULTS**

Commons Attribution NonCommercial (CC BY-NC 4.0) license, which permits others to distribute, remix, adapt, build upon this work non-commercially, and license their derivative works on different terms, provided the original work is properly cited and the use is non-commercial. See: <http://creativecommons.org/licenses/by-nc/4.0/>

**Manuscript source:** Unsolicited manuscript

**Specialty type:** Gastroenterology and hepatology

**Country/Territory of origin:** China

**Peer-review report's scientific quality classification**

Grade A (Excellent): 0  
Grade B (Very good): 0  
Grade C (Good): C  
Grade D (Fair): 0  
Grade E (Poor): 0

**Received:** January 8, 2021

**Peer-review started:** January 8, 2021

**First decision:** February 11, 2021

**Revised:** February 14, 2021

**Accepted:** March 24, 2021

**Article in press:** March 24, 2021

**Published online:** April 28, 2021

**P-Reviewer:** Casella C

**S-Editor:** Gao CC

**L-Editor:** Filipodia

**P-Editor:** Li JH



Compared with the control group, CPI-455 significantly inhibited Eca-109 cell proliferation. Gemcitabine inhibited Eca-109 cell proliferation in a concentration- and time-dependent manner. CPI-455 caused extensive alteration of the mitochondria, which appeared to have become atrophied. The cell membrane was weakly stained and the cytoplasmic structures were indistinct and disorganized, with serious cavitation when viewed by transmission electron microscopy. The flow cytometry and western blot results showed that, compared with the control group, the mitochondrial membrane potential was decreased and depolarized in Eca-109 cells treated with CPI-455. CPI-455 significantly upregulated the ROS content, P53, Bax, Caspase-9, and Caspase-3 protein expression in Eca-109 cells, whereas KDM5C expression was downregulated.

## CONCLUSION

CPI-455 inhibited Eca-109 cell proliferation *via* mitochondrial apoptosis by regulating the expression of related genes.

**Key Words:** Lysine-specific demethylase 5C; CPI-455; Esophageal squamous cell carcinoma; Caspase; P53

©The Author(s) 2021. Published by Baishideng Publishing Group Inc. All rights reserved.

**Core Tip:** This study confirmed that the lysine demethylase 5C inhibitor CPI-455 inhibited the proliferation of Eca-109 esophageal squamous cell carcinoma cells. CPI-455 played a role in esophageal squamous cell carcinoma cells proliferation and invasion that may have been associated in part with p53, Bax, Caspase-9, and Caspase-3 expression. CPI-455 induced Eca-109 cell apoptosis *via* a mitochondria-mediated intrinsic apoptotic signaling pathway by regulating the expression of related genes.

**Citation:** Xue XJ, Li FR, Yu J. Mitochondrial pathway of the lysine demethylase 5C inhibitor CPI-455 in the Eca-109 esophageal squamous cell carcinoma cell line. *World J Gastroenterol* 2021; 27(16): 1805-1815

**URL:** <https://www.wjgnet.com/1007-9327/full/v27/i16/1805.htm>

**DOI:** <https://dx.doi.org/10.3748/wjg.v27.i16.1805>

## INTRODUCTION

Esophageal cancer is a common digestive tract cancer, of which esophageal squamous cell carcinoma (ESCC) and esophageal adenocarcinoma represent the main histological types<sup>[1,2]</sup>. The incidence of esophageal cancer is relatively high, ranking seventh worldwide. ESCC accounts for more than 90% of esophageal cancers. As it is difficult to diagnose ESCC early due to a lack of specific clinical symptoms and insufficient preventive measures, it is often diagnosed at an advanced stage and has a poor prognosis. In addition, the 5-yr postoperative survival rate is less than 50%<sup>[3-5]</sup>. The lysine-specific demethylase 5C (KDM5C) inhibitor, CPI-455, regulates the apoptosis and proliferation of tumor cells by regulating the methylation state of lysine in KDM5C<sup>[6]</sup>. CPI-455 activity been reported in cervical<sup>[7]</sup>, gastric<sup>[8]</sup>, and prostate cancer<sup>[9]</sup>, and in other diseases<sup>[10,11]</sup>; but not in the treatment of esophageal cancer. In this study, human ESCC Eca-109 cells were used as a research model to preliminarily study the effect and mechanism of CPI-455 against ESCC and to explore novel approaches for the treatment and prevention of ESCC.

## MATERIALS AND METHODS

### Cell lines

Eca-109 human esophageal cancer cells and HPT-1A normal human esophageal epithelial cells were provided by the Cell Resource Center of the Shanghai Life Sciences Institute, Chinese Academy of Sciences (Shanghai, China). Other materials

included CPI-455 (MSDS, 1628208-23-0; Gibco, Ltd., United States), DMEM and RPMI 1640 cell culture media and fetal bovine serum (Gibco, Ltd). Anti-human P53 (cat no. sc-6243), Bax, KDM5C (cat no. sc-81623), Caspase-9 (cat no. 9746), Caspase-3 (cat no. 9502), GAPDH (glyceraldehyde-3-phosphate dehydrogenase, cat no. sc-47778) polyclonal antibody (1:200; Abcam, United Kingdom) were used for western blotting. Annexin V-fluorescein isothiocyanate (FITC)/propidium iodide (PI) apoptosis detection kits (cat no. F7250) were from Sigma-Aldrich (United States). polyvinylidene difluoride (PVDF) membranes were from Biyuntian Biotech (China) and bicinchoninic acid (BCA) protein quantitative detection kits were from Thermo Fisher (United States). An Epics Ultra flow cytometer (Beckman Coulter, United States), JEM-100sx transmission electron microscope (Jeol Ltd., Japan), and a TCS SP2 laser confocal microscope (Leica, Germany) were used.

### **Cell culture**

Eca-109 cells were cultured in DMEM and HET-1A cells were cultured in RPIM-1640 medium. Both were supplemented with 10% pre-inactivated FBS, 100 U/mL penicillin, and 100 U/mL streptomycin. Cells were adherently cultured in a 37 °C constant temperature incubator with a volume fraction of 5% CO<sub>2</sub> and 95% humidity; 0.25% trypsin-EDTA was used for cell digestion and passage. Cell growth in the culture flask was observed every 1-2 d, and the cell culture medium was replaced for passage culture.

### **Methyl tetrazolium assay**

For assay of growth and the logarithmic phase, cells were collected by trypsin digestion and centrifugation and 90 mL of a single cell suspension ( $3 \times 10^3$ /mL) were inoculated into 96-well culture plates and cultured at 37 °C in an atmosphere containing 5% CO<sub>2</sub> overnight to ensure adherence. When the cells grew to the appropriate density, the supernatant was discarded and 100 mL of the CPI-455 KDM5C inhibitor was added to each well, giving a final concentration of 15 mmol/L. The plates were cultured in an atmosphere containing 5% CO<sub>2</sub> at 37 °C for 0, 24, 48, 72, and 96 h (5 wells/time point). Following this, the cells were collected and centrifuged at 150 g for 10 min. The supernatant was discarded and the precipitate was washed once with phosphate buffered saline (PBS). A total of 200 µL of serum-free RPMI-1640 medium was added, followed by addition of 10 µL of methyl tetrazolium (MTT; 5 mg/mL). Following culture for a further 4 h, the supernatant was removed and 150 µL DMSO was added to each well to dissolve the purple crystals. The optical density (OD) was read at 490 nm after the crystals had completely dissolved. The survival rate was calculated as  $S\% = (\text{OD of the experimental group} / \text{OD of the control group}) \times 100$ .

### **Laser confocal scanning microscope assay of the ectropion of membrane phosphatidylserine**

The fluorescence of cell smears and suspension cultures after polylysine treatment was observed by confocal microscopy. Red (488/590 + 42 nm) and green (488/530 + 30 nm) dual channel detection and differential interference contrast imaging were performed. A total of 100 fields of vision were screened and 30 typical fields of vision were selected for inclusion in the preliminary statistical analysis. Annexin V-FITC (fluorescein isothiocyanate), PI double staining was performed and the fluorescence of Eca-109 cell membranes and necrotic nuclei was observed and analyzed as described above. DAPI (4', 6-diamidino-2-phenylindole, dihydrochloride) was used to stain the nuclei in cell smears and glycerol patches and analyzed by fluorescence microscopy, as described above.

### **Terminal deoxynucleotidyl transferase dUTP nick end labeling (TUNEL) assay of nucleation and DNA fragmentation of Eca-109 cells**

Eca-109 cells ( $5 \times 10^6$ /mL) were seeded in 24-well plates and cultured for 48 h. Cell smears were prepared from 50 µL of cell suspension on polylysine-treated slides that were fixed with 4% paraformaldehyde at room temperature for 30-60 min and washed twice with PBS. After treatment with terminal deoxynucleotidyl transferase and termination, the preparations were washed four times with PBS and incubated with FITC-labeled antibody for 30 min. Nuclei were stained with PI (1.0 g/mL) and the preparations were sealed with glycerin-mounted coverslips and marked. The cells were observed with a confocal laser scanning microscope, with FITC and PI dual channel fluorescence at an excitation wavelength of 490 nm and an emitted wavelength of 520 nm).

**Flow cytometry assay of reactive oxygen species (ROS)**

Eca-109 cells were cultured in a six-well plates ( $3 \times 10^3$  cells/well), treated with 15  $\mu\text{mol/L}$  CPI-455 for 48 h, and collected. The cells were washed three times in PBS, centrifuged for 5 min, and the supernatant was discarded. The cells were resuspended in serum-free medium, dichloro-dihydro-fluorescein diacetate (DCFH-DA) was added to a final concentration of 10  $\text{mmol/L}$ , and the plates were incubated at 37 °C for 40 min. The cells were centrifuged for 10 min, and the pellet was collected, washed, and resuspended in precooled PBS. The cells were centrifuged to obtain a pellet and were stained for fluorescence detection. Each assay was performed in triplicate.

**Flow cytometry assay of mitochondrial membrane potential**

Cells were harvested ( $2 \times 10^6/\text{mL}$ ) at scheduled times after treatment with 15  $\mu\text{mol/L}$  CPI-455 for 48 h. The Mitocapture dye and antibody incubation solutions were freshly prepared. The cells were washed and centrifuged and the mitochondria were stained. The cells were immediately transferred to collecting tubes for flow cytometry.

**Western blotting assay of P53, Bax, KDM5C, cleaved Caspase-9, and cleaved Caspase-3**

Eca-109 cells were cultured for 48 h, collected, and centrifuged at 150  $g$  for 5 min ( $r = 6$  cm). Total protein was extracted using a protein extraction kit. The supernatant was collected, and the protein concentration was determined using a BCA protein kit. Proteins were separated by sodium dodecyl sulfate-polyacrylamide gel electrophoresis (SDS-PAGE) and transferred to PVDF membranes. After blocking in 5% skim milk at room temperature for 2 h, anti-human mouse P53, Bax, KDM5C, Caspase-9, Caspase-3, and GAPDH monoclonal antibodies (1:1000; Santa Cruz Biotechnology, Inc., United States) were added and the membranes were incubated overnight at 4 °C and then with horseradish peroxidase (HRP)-labeled mouse secondary antibody (1:3,000; Origene Technologies Inc., China). The films were developed, fixed, scanned and analyzed using Image J software to calculate the gray values. Protein expression of the target protein was reported relative to GAPDH protein expression.

**Statistical analysis**

GraphPad Prism 6.0 software was used to statistical analyze the data. The data were reported as means  $\pm$  SD. All assays were repeated independently three times. Between-group differences were compared with independent samples *t*-tests. One-way analysis of variance was used to compare data with normal distributions. Least significant difference (LSD)-*t*-tests were used for pairwise comparisons of multiple groups. The significance level was = 0.05.

---

**RESULTS**

---

**CPI-455 inhibits Eca-109 cell proliferation**

The MTT results demonstrated that CPI-455 significantly inhibited the proliferation of Eca-109 cells in a time- and a concentration-dependent manner. The CPI-455 LD<sub>50</sub> was 15  $\text{mol/L}$  CPI-455 at 48 h. Therefore, the 48 h concentration of 15  $\text{mol/L}$  CPI-455 was selected for the follow-up procedures (Figure 1).

**CPI-455 induces Eca-109 cell apoptosis**

The laser confocal scanning microscopy results showed that prior to CPI-455 treatment, the Eca-109 cells had developed a complete mitochondrial structure. Mitocapture revealed a bright red color and "pipe-like network" that surrounded the nuclear lobule and was distributed throughout the entire cell. Following treatment with CPI-455 (15  $\mu\text{mol/L}$ ) for 48 h, both groups showed the presence of dye in the cytoplasm, with red mitochondrial staining and green cytoplasmic staining. Some cells contained visible "point and flake" red-stained mitochondria scattered in the cytoplasm, not present in clusters surrounding the nucleus, and gradually merging to form a "structureless aggregation". Substantial changes to the mitochondrial structure were observed, which appeared to indicate mitochondrial atrophy. Following CPI-455 treatment, the Eca-109 cell membranes were weakly stained and the internal cytoplasmic structures indistinct and disorganized, with severe cavitation (Figure 2A and B).

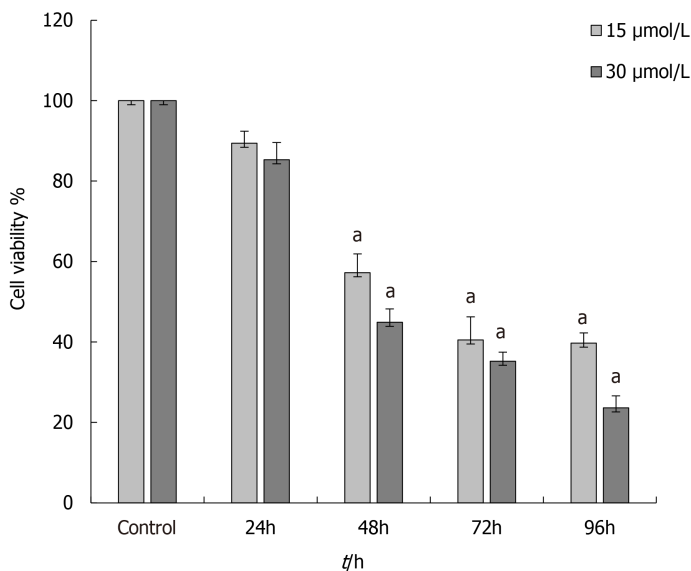


**Figure 1** Eca-109 cell viability following treatment with CPI-455 at different times and concentrations. Data are expressed as means  $\pm$  SE ( $n = 3$ ). <sup>a</sup> $P < 0.05$  vs control.

TUNEL and laser confocal scanning microscopy showed green fluorescence generated by the combination of FITC and the staining of 3'-OH terminal fragments produced by DNA fragmentation in the nucleus of apoptotic cells. Red fluorescence was emitted by PI-stained nuclei, which revealed the location of cells. Double-positive cells were seen in cells treated with CPI-455. Most Eca-109 cells in the CPI-455 group were double-positive for FITC and PI fluorescence. Most Eca-109 cells in the control group were negative for FITC and positive for PI, indicating that TUNEL assay of the CPI-455-stimulated group was positive. In terms of cell morphology, compared with the control group, most Eca-109 cells in the control group had a lower nuclear staining density, an unclear nuclear boundary, and larger nuclei. However, most ECA-109 cells in gemcitabine group had dense chromatin and small nuclei (Figure 2C and D).

### **CPI-455 upregulates ROS content, P53, Bax, Caspase-9, and Caspase-3 expression and downregulates KDM5C expression and mitochondrial membrane potential in Eca-109 cells**

Flow cytometry was used to detect the effect of CPI-455 on the level of ROS in Eca-109 cells. With an extension of the induction time, the level of intracellular ROS in the Eca-109 cells was increased significantly, with statistically significant differences observed at 24, 48, and 72 h ( $P < 0.01$ , Figure 3). Compared with the control group, the mitochondrial membrane potential was depolarized and decreased ( $P < 0.01$ , Figure 4). The western blot results found increased expression of p53, Bax, Caspase-9, and Caspase-3 at 24, 48, and 72 h following CPI-455 treatment (Figure 5). However, KDM5C protein expression in the treated cells was significantly decreased compared with the controls ( $P < 0.01$ , Figure 6).

## **DISCUSSION**

Esophageal cancer is a digestive tract malignant tumor that is difficult to diagnose early. The most common treatments are surgery, radiotherapy, chemotherapy, and biologically targeted therapy<sup>[12]</sup>. The prognosis remains poor. The occurrence and development of esophageal cancer is complex and involves multiple gene changes, commonly resulting from histone methylation and epigenetic regulation of tumor-related genes.

CPI-455 is a KDM5C inhibitor that modulates the apoptosis and proliferation of tumor cells by regulating the lysine methylation status KDM5C. Recent reports have confirmed that the anti-tumor effect of CPI-455 in ovarian, breast, stomach, lung, and liver cancer is achieved by inducing the apoptosis and autophagy of tumor cells *via* modulating KDM5C gene transcription and expression<sup>[13,14]</sup>. In this study, the anti-Eca-109 effect of CPI-455 was studied and the associated mechanism was explored.

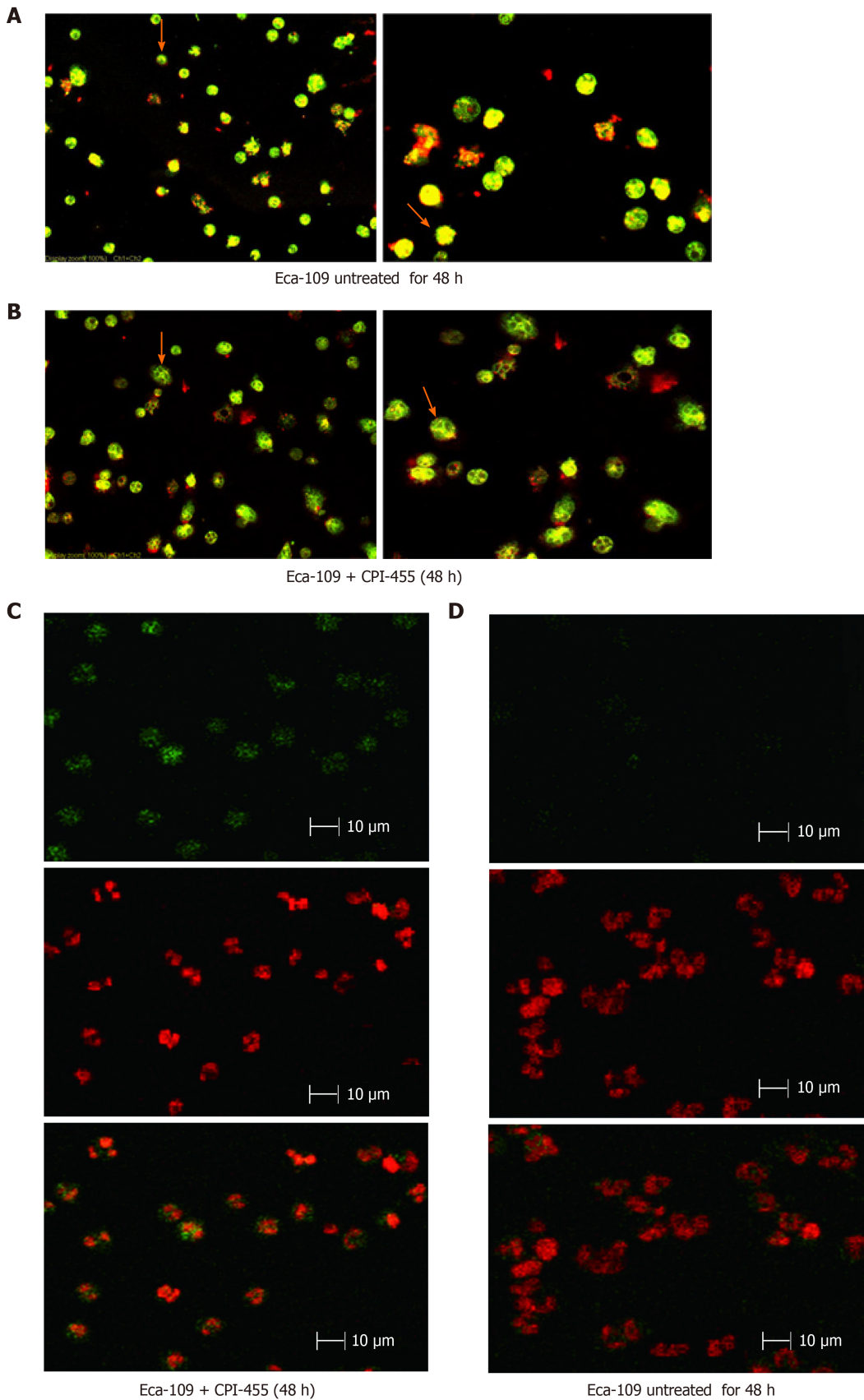


**Figure 2** Changes in Eca109 cells after 48 h culture with and without CPI-455 treatment. Left panels show the morphology of the mitochondria of Eca109 cells. A: Arrows indicate mitochondria with complete and clear structure. B: Arrows indicate mitochondria with a fuzzy structure and weak staining of cells. Right panels show TUNEL assay results (bar = 10  $\mu$ m) and laser confocal scanning microscopy  $\times$  600 of nuclear staining and DNA fragmentation of Eca109 cells C: without, and D: with CPI-455 treatment. Data are reported as means  $\pm$  SE ( $n = 3$ ).

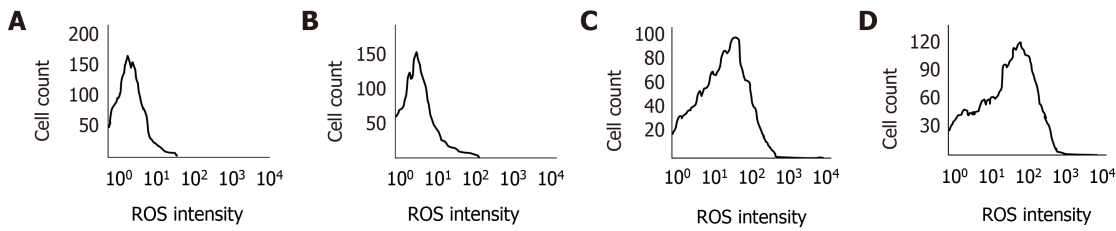


**Figure 3** Eca-109 induced by CPI-455 is dependent on the generation of reactive oxygen species. A: Eca109 untreated (0 h); B: Eca-109 induced by CPI-455 for 24 h; C: Eca-109 induced by CPI-455 for 48 h; D: Eca-109 induced by CPI-455 for 72 h. Data are reported as means  $\pm$  SE ( $n = 3$ ). ROS: Reactive oxygen species.

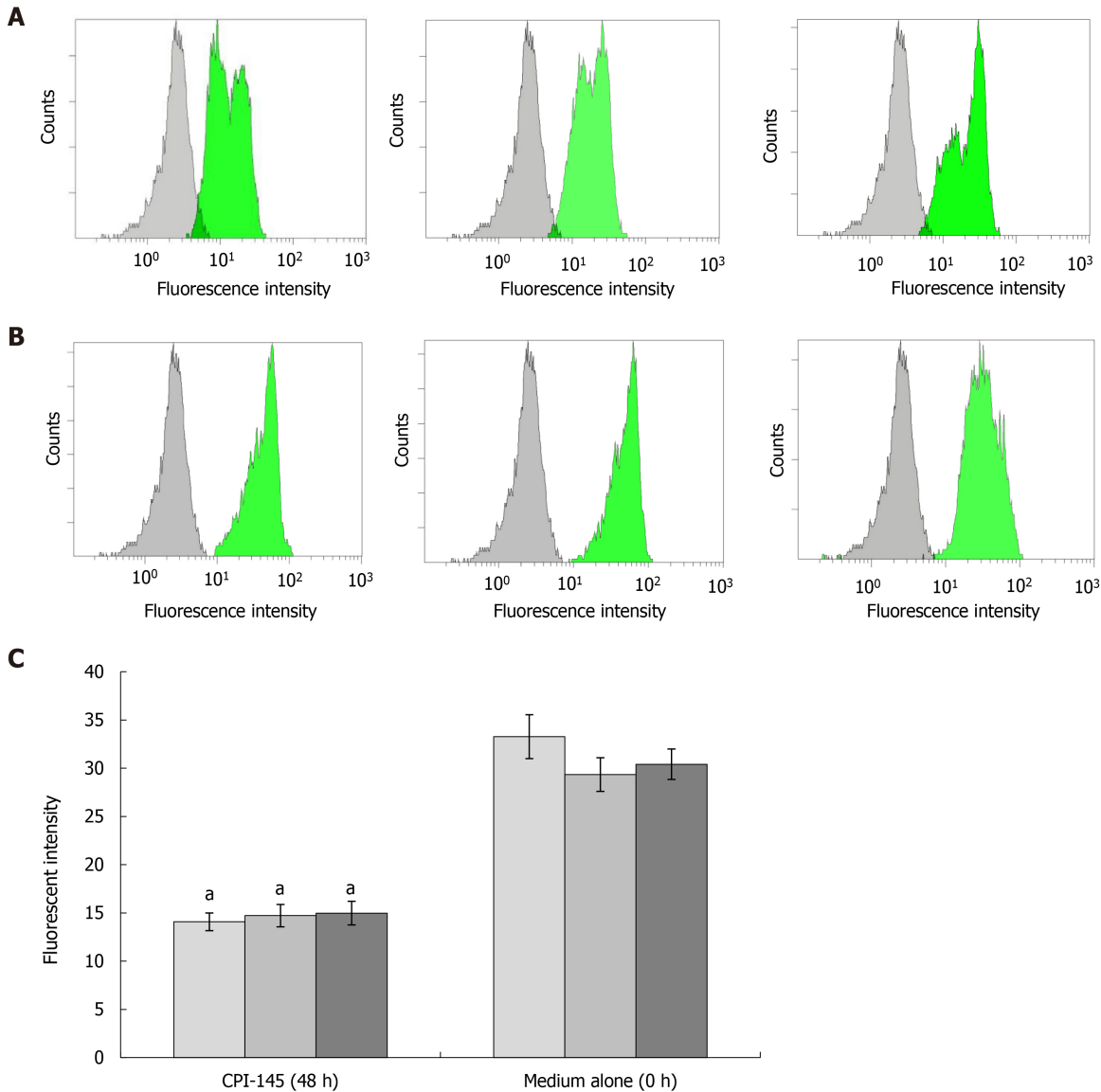


**Figure 4** Mitochondrial membrane potential assayed by flow cytometry. A: Eca109 untreated (0 h); B: Eca109 treated with CPI-455 for 48 h; C: Gray scale results of membrane potential energy of mitochondria (Blue: Results of the first assay; Red: Results of the second assay; Green: Results of the third assay). Data are reported as means  $\pm$  SE ( $n = 3$ ). <sup>a</sup> $P < 0.05$  vs control.

The study results found that CPI-455 inhibited the proliferation of esophageal cancer cells in a time-and concentration-dependent manner. However, at its effective concentration, CPI-455 was less toxic to normal esophageal cells than to Eca-109 cells. The inhibitory effect of CPI-455 on Eca-109 cell proliferation was confirmed by the assay of cell-membrane permeability by laser confocal scanning microscopy. This finding indicates that CPI-455 has favorable effects by inhibiting Eca-109 cell

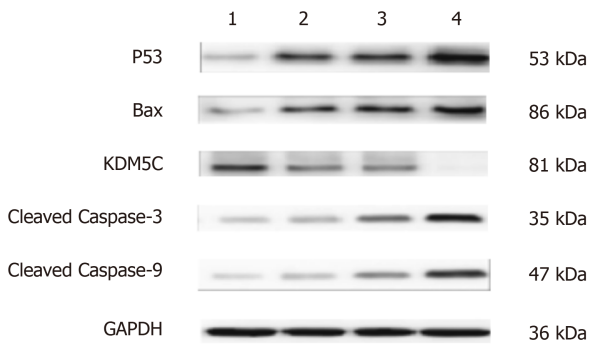


**Figure 5** Western blot assays of p53, Bax, lysine-specific demethylase 5C, cleaved Caspase 3, and cleaved Caspase 9 protein expression in Eca-109 cells. Lane 1: Eca109 untreated (0 h); Lane 2: Eca109 induced by CPI-455 for 24 h; Lane 3: Eca109 induced by CPI-455 for 48 h; Lane 4: Eca109 induced by CPI-455 for 72h. KDM5C: Lysine-specific demethylase 5C; GAPDH: Glyceraldehyde-3-phosphate dehydrogenase.

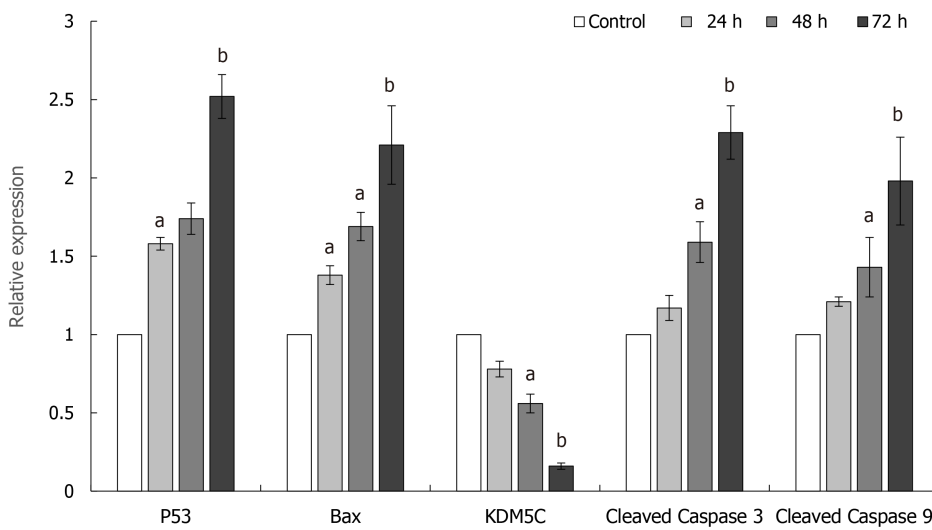


**Figure 6** Densitometry analysis of the immunoblotting data of P53, Bax, lysine-specific demethylase 5C, cleaved Caspase 3, and cleaved Caspase 9 proteins in Eca-109 cells. Data are reported as means ± SE (n = 3). <sup>a</sup>P < 0.05 vs control; <sup>b</sup>P < 0.01 vs control.

proliferation and growth, as well as the selective killing on ESCC cells (Figures 1 and 2).

Flow cytometry was used to determine the ROS content of Eca-109 cells, which is considered to be the by-product of oxygen consumption and cell metabolism. Previous studies have found that various chemotherapy drugs can induce an increase in the ROS content in tumor cells, and that at a certain level, ROS can induce the apoptosis of tumor cells<sup>[15-18]</sup>. Decrease of the mitochondrial membrane potential is the initial manifestation of the hypoxia apoptosis cascade<sup>[19]</sup>. In this study, the level of intracellular ROS significantly increased in treated Eca-109 cells (Figure 3), and depolarization of mitochondrial membrane was increased compared with controls (Figure 4). CPI-455 significantly induced the apoptosis of Eca-109 cells.

Previous studies have confirmed that the mechanism by which tumor cell apoptosis is induced varies widely depending on the various pathways that are involved. These includes mitochondrial pathways, which play an important role in the maintenance of stability, and those involving activation of multiple upstream and downstream genes (e.g., p53 and Bax). Activation of Caspase-2, 3, and 9 on the mitochondrial membrane is linked to the activation of mitochondrial apoptotic pathways<sup>[22-24]</sup>.

Therefore, the inhibitory effect of the KDM5C inhibitor, CPI-455, on Eca-109 cell proliferation may be related to the downregulation of KDM5C expression, activation of Caspase-3 and Caspase-9, change in mitochondrial membrane permeability, promotion of ROS production, depolarization of the mitochondrial membrane, release of the proapoptotic proteins, Bax and p53, in the mitochondria into the cytoplasm, and induction of tumor cell apoptosis (Figures 5 and 6). The above results indicate that CPI-455 induced apoptosis through an ROS-dependent mitochondrial signaling



pathway<sup>[25]</sup>.

Our study had some limitations, the mechanism involved in inducing apoptosis of tumor cells is extensive, and the mitochondrial apoptosis pathway is only one of them that plays an important role in maintaining cell stability. The mechanism has not been fully elucidated and needs further study. The results of this study provide a theoretical basis for the application of CPI-455 for the treatment of ESCC.

---

## CONCLUSION

---

CPI-455 inhibited ECA-109 cell proliferation *via* the mitochondrial apoptosis pathway by regulating the expression of related genes.

## ARTICLE HIGHLIGHTS

### **Research background**

Esophageal cancer is a malignant tumor of the digestive tract that is difficult to diagnose early. Although CPI-455 is reported to inhibit various cancers, the role of CPI-455 in esophageal squamous cell carcinoma (ESCC) is unknown.

### **Research motivation**

KDM5C, a lysine-specific demethylase 5C, inhibited ESCC proliferation and invasion, which may be partly associated with the expression of p53, Bax, Caspase-9, and Caspase-3. Mitochondria-mediated intrinsic apoptotic signaling plays an important role in the process of Eca-109 cell apoptosis induced by CPI-455.

### **Research objectives**

The study objective was to investigate the effect and mechanism of the KDM5C inhibitor, CPI-455, on ESCC cells.

### **Research methods**

The changes in proliferation, apoptosis, ROS content, and mitochondrial membrane potential of Eca-109 cells induced by CPI-455 were observed. The expression of P53, Bax, Caspase-9, Caspase-3, and KDM5C in Eca-109 cells was assayed.

### **Research results**

CPI-455 inhibited Eca-109 cell proliferation. P53, Bax, Caspase-9, and Caspase-3 were upregulated in Eca-109 cells, and KDM5C was significantly downregulated, by CPI-455. CPI-455 increased the level of intracellular ROS in Eca-109 cells, and decreased the mitochondrial membrane potential compared with the control group.

### **Research conclusions**

CPI-455 inhibited Eca-109 cell proliferation *via* the mitochondrial apoptosis pathway by regulating the expression of related genes.

### **Research perspectives**

CPI-455 might be a potential candidate for the development of novel chemotherapeutic agents to treat ESCC.

---

## ACKNOWLEDGEMENTS

---

We thank all the members of Department of Clinical Laboratory, Huangshi Central Hospital, Affiliated Hospital of Hubei Polytechnic University, Edong Healthcare Group and Department of Laboratory Medicine, Hubei cancer hospital, Tongji Medical College, Huazhong University of Science and Technology.

## REFERENCES

- 1 **Samson P**, Lockhart AC. Biologic therapy in esophageal and gastric malignancies: current therapies and future directions. *J Gastrointest Oncol* 2017; **8**: 418-429 [PMID: 28736629 DOI: 10.21037/jgo.2016.11.13]
- 2 **Feng RM**, Zong YN, Cao SM, Xu RH. Current cancer situation in China: good or bad news from the 2018 Global Cancer Statistics? *Cancer Commun (Lond)* 2019; **39**: 22 [PMID: 31030667 DOI: 10.1186/s40880-019-0368-6]
- 3 **Sohda M**, Kuwano H. Current Status and Future Prospects for Esophageal Cancer Treatment. *Ann Thorac Cardiovasc Surg* 2017; **23**: 1-11 [PMID: 28003586 DOI: 10.5761/ates.ra.16-00162]
- 4 **Yan CY**, Chen LQ. [Retrospect of 2019: focus on the surgical treatment for adenocarcinoma of esophagogastric junction]. *Zhonghua Wei Chang Wai Ke Za Zhi* 2020; **23**: 20-25 [PMID: 31958926 DOI: 10.3760/cma.j.issn.1671-0274.2020.01.004]
- 5 **Abbas G**, Krasna M. Overview of esophageal cancer. *Ann Cardiothorac Surg* 2017; **6**: 131-136 [PMID: 28447001 DOI: 10.21037/acs.2017.03.03]
- 6 **Fu YD**, Huang MJ, Guo JW, You YZ, Liu HM, Huang LH, Yu B. Targeting histone demethylase KDM5B for cancer treatment. *Eur J Med Chem* 2020; **208**: 112760 [PMID: 32883639 DOI: 10.1016/j.ejmech.2020.112760]
- 7 **Zhang Y**, Li X, Zhang J, Mao L. E6 hijacks KDM5C/Lnc\_000231/miR-497-5p/CCNE1 axis to promote cervical cancer progression. *J Cell Mol Med* 2020; **24**: 11422-11433 [PMID: 32818316 DOI: 10.1111/jcmm.15746]
- 8 **Xu L**, Wu W, Cheng G, Qian M, Hu K, Yin G, Wang S. Enhancement of Proliferation and Invasion of Gastric Cancer Cell by KDM5C Via Decrease in p53 Expression. *Technol Cancer Res Treat* 2017; **16**: 141-149 [PMID: 26858085 DOI: 10.1177/1533034616629261]
- 9 **Hong Z**, Wu G, Xiang ZD, Xu CD, Huang SS, Li C, Shi L, Wu DL. KDM5C is transcriptionally regulated by BRD4 and promotes castration-resistance prostate cancer cell proliferation by repressing PTEN. *Biomed Pharmacother* 2019; **114**: 108793 [PMID: 30921702 DOI: 10.1016/j.biopha.2019.108793]
- 10 **Talebizadeh Z**, Shah A, DiTacchio L. The potential role of a retrotransposed gene and a long noncoding RNA in regulating an X-linked chromatin gene (KDM5C): Novel epigenetic mechanism in autism. *Autism Res* 2019; **12**: 1007-1021 [PMID: 31087518 DOI: 10.1002/aur.2116]
- 11 **Wei G**, Deng X, Agarwal S, Iwase S, Distechi C, Xu J. Patient Mutations of the Intellectual Disability Gene KDM5C Downregulate Netrin G2 and Suppress Neurite Growth in Neuro2a Cells. *J Mol Neurosci* 2016; **60**: 33-45 [PMID: 27421841 DOI: 10.1007/s12031-016-0770-3]
- 12 **Hirano H**, Kato K. Systemic treatment of advanced esophageal squamous cell carcinoma: chemotherapy, molecular-targeting therapy and immunotherapy. *Jpn J Clin Oncol* 2019; **49**: 412-420 [PMID: 30920626 DOI: 10.1093/jjco/hyz034]
- 13 **Peng Y**, Alexov E. Cofactors-loaded quaternary structure of lysine-specific demethylase 5C (KDM5C) protein: Computational model. *Proteins* 2016; **84**: 1797-1809 [PMID: 27696497 DOI: 10.1002/prot.25162]
- 14 **Denis H**, Van Grembergen O, Delatte B, Dedeurwaerder S, Putmans P, Calonne E, Rothé F, Sotiriou C, Fuks F, Deplus R. MicroRNAs regulate KDM5 histone demethylases in breast cancer cells. *Mol Biosyst* 2016; **12**: 404-413 [PMID: 26621457 DOI: 10.1039/c5mb00513b]
- 15 **Bertero E**, Maack C. Calcium Signaling and Reactive Oxygen Species in Mitochondria. *Circ Res* 2018; **122**: 1460-1478 [PMID: 29748369 DOI: 10.1161/CIRCRESAHA.118.310082]
- 16 **Zhelev Z**, Ivanova D, Bakalova R, Aoki I, Higashi T. Inhibition of the Pentose-phosphate Pathway Selectively Sensitizes Leukemia Lymphocytes to Chemotherapeutics by ROS-independent Mechanism. *Anticancer Res* 2016; **36**: 6011-6020 [PMID: 27793928 DOI: 10.21873/anticancer.11190]
- 17 **Shen J**, Li ZJ, Hang ZF, Xu SF, Liu QQ, Tang H, Zhao XW. Insights into the Effect of Reactive Oxygen Species Regulation on Photocatalytic Performance via Construction of a Metal-Semiconductor Heterojunction. *J Nanosci Nanotechnol* 2020; **20**: 3478-3485 [PMID: 31748041 DOI: 10.1166/jnn.2020.17405]
- 18 **Shukla H**, Chitrakar R, Bibi HA, Gaje G, Koucheqi A, Trush MA, Zhu H, Li YR, Jia Z. Reactive oxygen species production by BP-1,6-quinone and its effects on the endothelial dysfunction: Involvement of the mitochondria. *Toxicol Lett* 2020; **322**: 120-130 [PMID: 31953210 DOI: 10.1016/j.toxlet.2020.01.011]
- 19 **Chan CK**, Supriady H, Goh BH, Kadir HA. Elephantopus scaber induces apoptosis through ROS-dependent mitochondrial signaling pathway in HCT116 human colorectal carcinoma cells. *J Ethnopharmacol* 2015; **168**: 291-304 [PMID: 25861953 DOI: 10.1016/j.jep.2015.03.072]
- 20 **Chamani E**, Rezaei Z, Dastjerdi K, Javanshir S, Khorsandi K, Mohammadi GA. Evaluation of some genes and proteins involved in apoptosis on human chronic myeloid leukemia cells (K562 cells) by *datura innoxia* leaves aqueous extract. *J Biomol Struct Dyn* 2020; **38**: 4838-4849 [PMID: 31709925 DOI: 10.1080/07391102.2019.1691661]
- 21 **Eslami F**, Mahdavi M, Babaei E, Hussen BM, Mostafavi H, Shahbazi A, Hidayat HJ. Down-regulation of Survivin and Bcl-2 concomitant with the activation of caspase-3 as a mechanism of apoptotic death in KG1a and K562 cells upon exposure to a derivative from ciprofloxacin family. *Toxicol Appl Pharmacol* 2020; **409**: 115331 [PMID: 33171188 DOI: 10.1016/j.taap.2020.115331]
- 22 **An N**, Sun Y, Ma L, Shi S, Zheng X, Feng W, Shan Z, Han Y, Zhao L, Wu H. Helveticoside

- Exhibited p53-dependent Anticancer Activity Against Colorectal Cancer. *Arch Med Res* 2020; **51**: 224-232 [PMID: 32147288 DOI: 10.1016/j.arcmed.2020.02.007]
- 23 **Gao G**, Chang F, Zhang T, Huang X, Yu C, Hu Z, Ji M, Duan Y. Naringin Protects Against Interleukin 1 $\beta$  (IL-1 $\beta$ )-Induced Human Nucleus Pulposus Cells Degeneration *via* Downregulation Nuclear Factor kappa B (NF- $\kappa$ B) Pathway and p53 Expression. *Med Sci Monit* 2019; **25**: 9963-9972 [PMID: 31927560 DOI: 10.12659/MSM.918597]
  - 24 **Hou XF**, Xu LP, Song HY, Li S, Wu C, Wang JF. *ECRG2* enhances the anti-cancer effects of cisplatin in cisplatin-resistant esophageal cancer cells *via* upregulation of *p53* and downregulation of *PCNA*. *World J Gastroenterol* 2017; **23**: 1796-1803 [PMID: 28348485 DOI: 10.3748/wjg.v23.i10.1796]
  - 25 **Li J**, Wu DD, Zhang JX, Wang J, Ma JJ, Hu X, Dong WG. Mitochondrial pathway mediated by reactive oxygen species involvement in  $\alpha$ -hederin-induced apoptosis in hepatocellular carcinoma cells. *World J Gastroenterol* 2018; **24**: 1901-1910 [PMID: 29740205 DOI: 10.3748/wjg.v24.i17.1901]



Published by **Baishideng Publishing Group Inc**  
7041 Koll Center Parkway, Suite 160, Pleasanton, CA 94566, USA

**Telephone:** +1-925-3991568

**E-mail:** [bpgoffice@wjgnet.com](mailto:bpgoffice@wjgnet.com)

**Help Desk:** <https://www.f6publishing.com/helpdesk>

<https://www.wjgnet.com>

